PρT Behavior of a Lean Synthetic Natural Gas Mixture Using Magnetic Suspension Densimeters and an Isochoric Apparatus: Part I

M. Atilhan,*,† S. Aparicio,‡ S. Ejaz,§ D. Cristancho,§ and K. R. Hall§

Chemical Engineering Department, Qatar University, Qatar, Chemistry Department, University of Burgos, Spain, and Artie McFerrin Department of Chemical Engineering, Texas A&M University, College Station, Texas, United States

Work shown in this paper reports measurements of fluid behavior and its dependence upon concentration in natural gas-like mixtures. These systematic experiments covering phase equilibrium and densities of selected mixtures use a state-of-the art apparatus. This work presents phase envelopes and density data for a synthetic natural gas-like mixture measured with an isochoric apparatus and a magnetic suspension densimeter. The isochoric apparatus permits precise, fast measurements using an automated procedure over wide ranges of pressure and temperature encompassing the cricondentherm and the cricondenbar. A comparison of the measured phase envelopes to predictions from cubic and molecular-based equation of states (EOS's) indicate serious deviations in both cricondentherm and cricondenbar regions. Although most design software use these models, the results obtained here indicate the EOS predictions are unacceptable. Current density measurements deviate from both the AGA8-DC92 and the GERG-2004 models.

Background

Natural gas is the most environmentally friendly fossil fuel because it burns cleaner and more efficiently than coal or oil. Proven reserves of natural gas have increased yearly, and development of new technologies together with the current high prices of oil allows the exploration and recovery of nonconventional reservoirs whose compositions and characteristics are unusual.[1,2] Some of these sources provide gas that contains a significant fraction of heavy hydrocarbons. Most equations of state (EOS's) that purport to describe natural gas cannot match the phase envelopes for pressures above that of the cricondentherm nor can they match the high pressure density data.[3]

Natural gas compositions depend upon the age and conditions of the reservoir[4] and range from methane to long chain n-alkanes that strongly affect phase behavior, to quadrupolar molecules such as carbon dioxide, and molecules that can autoassociate through hydrogen bonding like hydrogen sulfide and water. These multicomponent mixtures contain complex intermolecular forces and related effects that make a theoretical description of the systems difficult. The prediction of phase equilibria commonly uses EOS's, but the marginal accuracy of these models[5] renders experimental measurements necessary to determine system properties. It is impossible to measure all of the properties for all possible mixtures over the temperature and pressure ranges required. The measurement of the required volumetric properties and vapor−liquid equilibrium in multicomponent mixtures requires high-pressure and wide temperature ranges for deep reservoir gas simulations. Measurements require experimental skill and state-of-the-art equipment and have financial and time constraints.[6,7] Considering the importance of experimental measurements and their difficulty, it is necessary to develop a systematic strategy from which to infer the effects of different mixture components and concentrations upon thermodynamic properties.

Accurate knowledge of phase envelopes is relevant for production, storage, processing, and transportation of natural gases.[8] Inaccurate dew point predictions may cause contractual disputes between the gas producers and the purchasers.[9] Different experimental designs have appeared for measurements of phase envelopes such as a visual equilibrium cell, microwave equipment, and surface acoustic techniques,[10−17] but the isochoric method is interesting because of its accuracy and ease of automation.[8,18,19] The use of an isochoric apparatus allows determination of points on the phase envelope and, when combined with density data obtained with a densimeter, produces density data along the isochores.[18]

Knowledge of the pressure−density−temperature ($p-\rho-T$) behavior of natural gas at reservoir and pipeline conditions is necessary for several practical applications, the most important of which is the metering of custody transfer of natural gas.[20] Simple models predict densities of natural gas in the custody transfer region within ± 1 % relative deviation with respect to reliable experimental data, which is not sufficient for custody transfer.[21,22] A modified version of the Redlich−Kwong (RK) EOS,[23,24] the Hall−Yarborough[25] correlation, and the models by Dranchuk et al.[26] and Dranchuk et al.[27] are other suggested EOS's. The gas industry uses cubic EOS's to predict phase envelopes since their ease of use and wide availability in commercial packages provide quick solutions and they do not require high computational requirements.[28,29] However, although these models are useful for some applications,[28] the uncertainty of their predictions[5] requires oversizing many industrial designs. Molecular-based EOS's have stronger theoretical foundations than cubic equations; however, practical use of these EOS's is limited by their complexity and computational speed.[30]

AGA8-DC92 (American Gas Association, Report No. 8, Washington, DC, 1992)[31] is the U.S. reference equation adopted by the American Gas Association for natural gas density predictions. Its validity is limited to well-known pressure,

* Corresponding author. E-mail: mert.atilhan@qu.edu.qa.
† Qatar University.
‡ University of Burgos.
§ Texas A&M University.

10.1021/je100676j
Published on Web 01/19/2011

Table 1. Mixture Mole Fractions

component	mole fraction
methane	0.89982
ethane	0.03009
propane	0.01506
2-methylpropane	0.00752
butane	0.00753
2-methylbutane	0.00300
pentane	0.00300
nitrogen	0.01697
carbon dioxide	0.01701

temperature, and composition ranges, and it is not applicable for phase equilibrium calculations or for liquid properties.[32,33] Current work calls into question the uncertainty bands proposed for AGA8-DC92.

This work contains the first results of a research project covering $p-\rho-T$ and phase behavior of multicomponent mixtures. The same mixtures were measured with a two-sinker densimeter at National Institute of Standards and Technology (NIST) at Boulder, and these data will be reported by McLinden in a future communication.[34]

Experimental Section

Materials. Accurate Gas, Inc. prepared the synthetic mixture used in this work, and its composition appears in Table 1. The gravimetrically prepared mixture has mass traceability to NIST. The overall uncertainty of the mixture has been estimated with 1σ as 0.12 % in molar weight (or 0.0222 kg·kmol^{-1}).

Isochoric Apparatus. Figures 1 and 2 are schematic diagrams of the overall isochoric apparatus and the measuring cell. Details of the isochoric apparatus appear in a previous work.[8] The isochoric apparatus operates between (100 and 500) K at pressures (up to 35 MPa) in a simple, automated manner. The technique for determining phase envelopes utilizes the change of the slope of an isochor as it crosses the phase boundary. A new technique developed by Pedro et al. is used to calculate exact points on the phase boundary.[35] Collinearity of the isochores was originally discovered by Doiron et al.[36] in 1976. Several methods for the detection of the phase boundary use a change of slope method, and the method we used in this paper for phase change detection uses the change of slope of isochors especially to detect the lower dew point curve. At higher densities approaching the cricondentherm, the method fails. Moreover, it also fails in the zero density limit; however, it still can be used again at high densities as well above the cricondentherm density. It is thermodynamically impossible for measured data to ever have an isochoric slope greater on the single-phase side of a lower dew-point envelope rather than on the two-phase side.[37,38] For our measurements of phase boundary points, we used the above techniques. We fitted the single phase isochoric data on one single equation, and at the vicinity of the phase envelope we kept on adding isochoric data point on the fitted equation and observed the isochoric slope jump at each case. Given the technique description, with this technique we are able to limit the uncertainty of the phase envelope measurements to $5\cdot10^{-4}\,p$ in pressure and 5 mK in temperature.

The volume of the isochoric cell is approximately 70 cm^3. Since the apparatus cell volume changes slightly with pressure and temperature, experimental runs are actually isomoles instead of isochores, and the data require a cell distortion correction to adjust the results to isochores:

$$\frac{V(T,P)}{V(T_0,P_0)} = 1 + \gamma(P - P_0) + \beta(T - T_0) \qquad (1)$$

in which T_0 and P_0 are the reference temperature and pressure points on an isochore line that are measured accurately[39] and cross-checked from *Roark's Formulas for Stress and Strain* book[40] for accurate values as $\gamma = 2.53\cdot10^{-5}$ MPa^{-1} and $\beta = 4.86\cdot10^{-5}$ K^{-1} for stainless steel. Circulating baths and surrounding heaters control the cell temperature, and the system

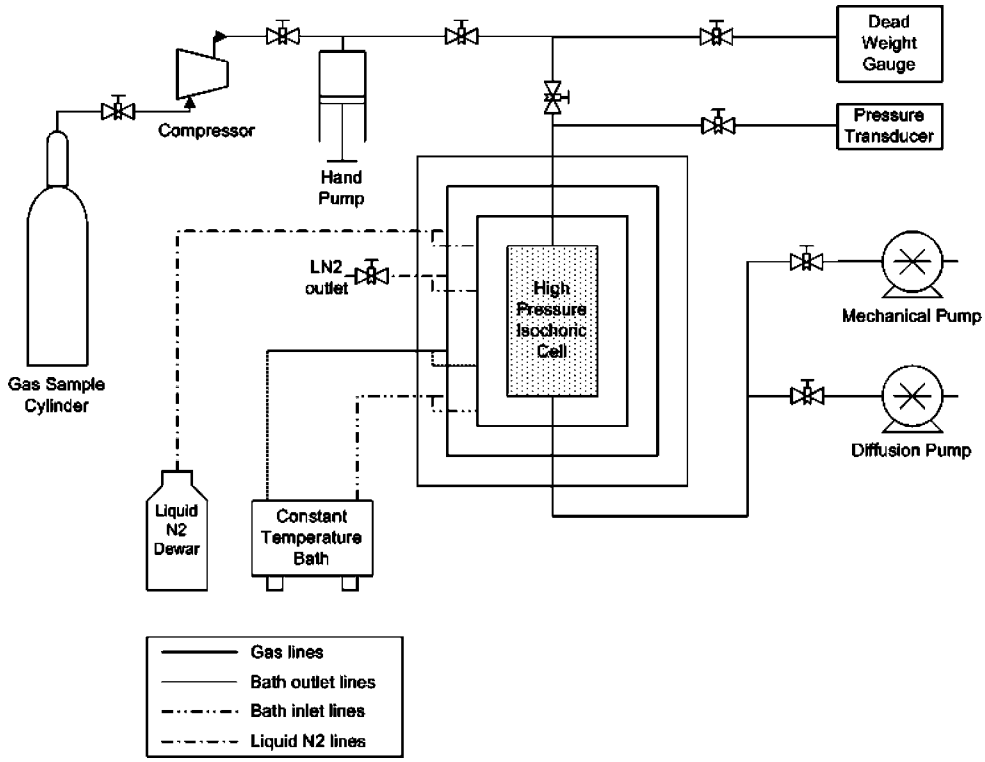

Figure 1. Block diagram of the isochoric apparatus.

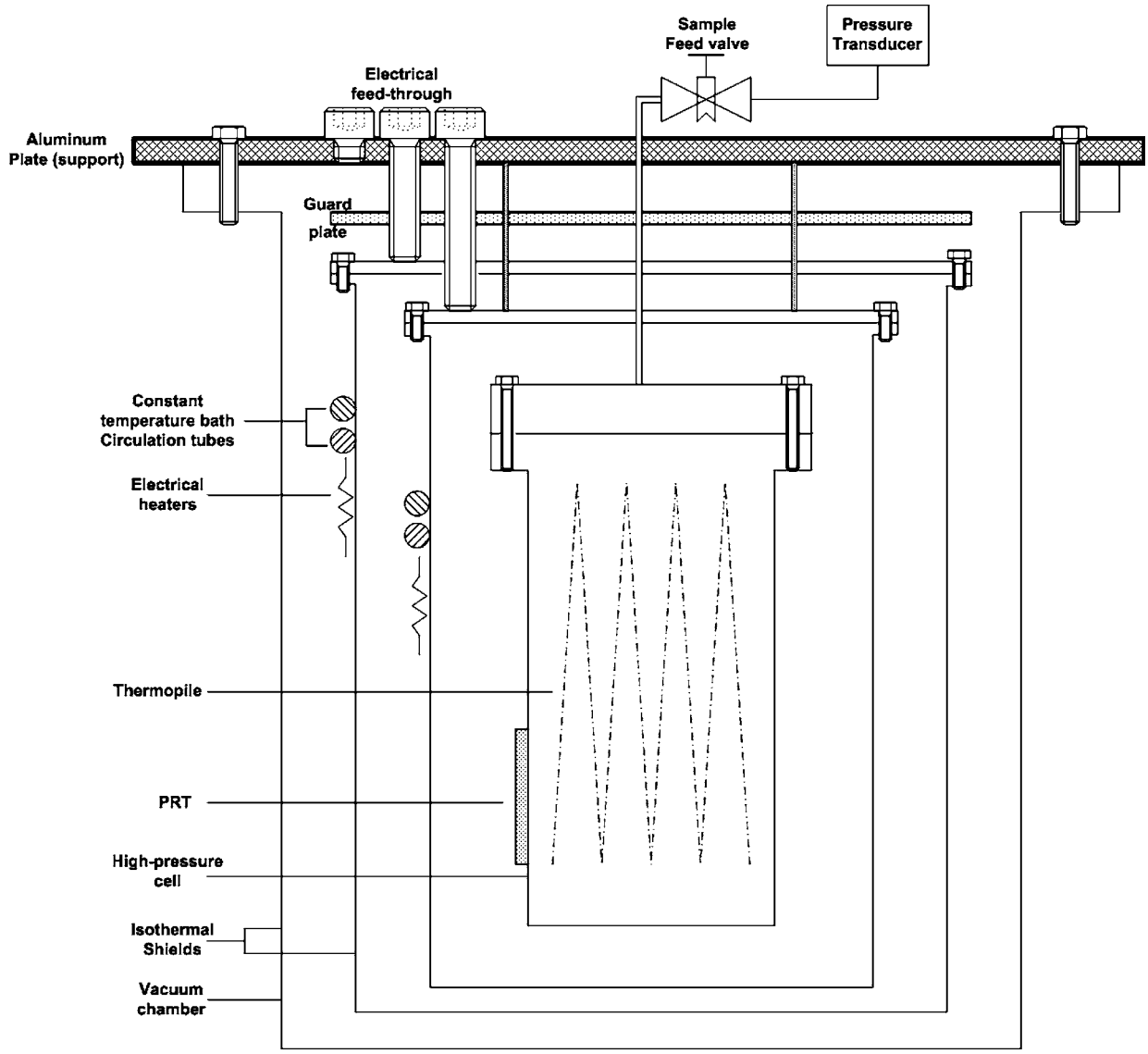

Figure 2. Schematic of the isochoric cell (liquid nitrogen and circulating bath tubes go in both isothermal shields).

uses isolating vacuum and radiation shields surrounding the cell to reduce energy transmission and to ensure temperature stability of the measurements within the cell as ± 5 mK measured via a platinum resistance thermometer. A quartz pressure transducer from Paroscientific Inc. measures pressure within the cell with a manufacturer specified relative uncertainty of ± 0.01 % of full scale or $1 \cdot 10^{-4}$ *p*. The transducer temperature is constant at 343.15 K during measurements, well above the mixture cricondentherm. A fully automated program that allows rapid collection of data controls the apparatus. The calibration of the pressure transducer was conducted also at the same temperature previously.

Magnetic Suspension Densimeter. Figure 3 shows the schematic diagram of the densimeter apparatus. This instrument use the hydrostatic buoyancy force technique based upon Archimedes' Principle. Archimedes' Principle states that "A solid body immersed in a fluid displaces a volume of fluid the weight of which equals the buoyancy force exerted by the fluid on the body." This observation relates the buoyancy force to the fluid density. Classical hydrostatic buoyancy densimeters suspend a sinker, usually a sphere or cylinder, from a commercial digital balance using a thin wire. The pressure and temperature of the fluid remain constant in the cell. The weight of the submerged sinker is measured, and the density of the fluid is:

$$\rho = \frac{m_v - m_a}{V_s(T,P)} \tag{2}$$

In eq 2, m_v is the "true" mass of the sinker in vacuum, m_a is the "apparent" mass of the sinker in the fluid, and V_s is the calibrated volume of the sinker, which is a function of temperature and pressure. In such densimeters, several corrections are necessary to reduce the effect of surface tension between the sample liquid and the immersed part of the wire and the effect of the buoyant force of air on the masses of the analytical balance. Zero shift of balance readings, buoyancy forces on auxiliary devices, adsorption effects, and surface tension may reduce the accuracy of such measurements. To overcome limitations in achievable accuracy, the need for frequent calibration of the apparatus with reference fluids, complexity of operation, and limitations on temperature and pressure, Kleinrahm and Wagner[41] introduced a magnetic-suspension device (MSD) which was initially developed by Beams and Clarke.[42] The novelty of the magnetic-

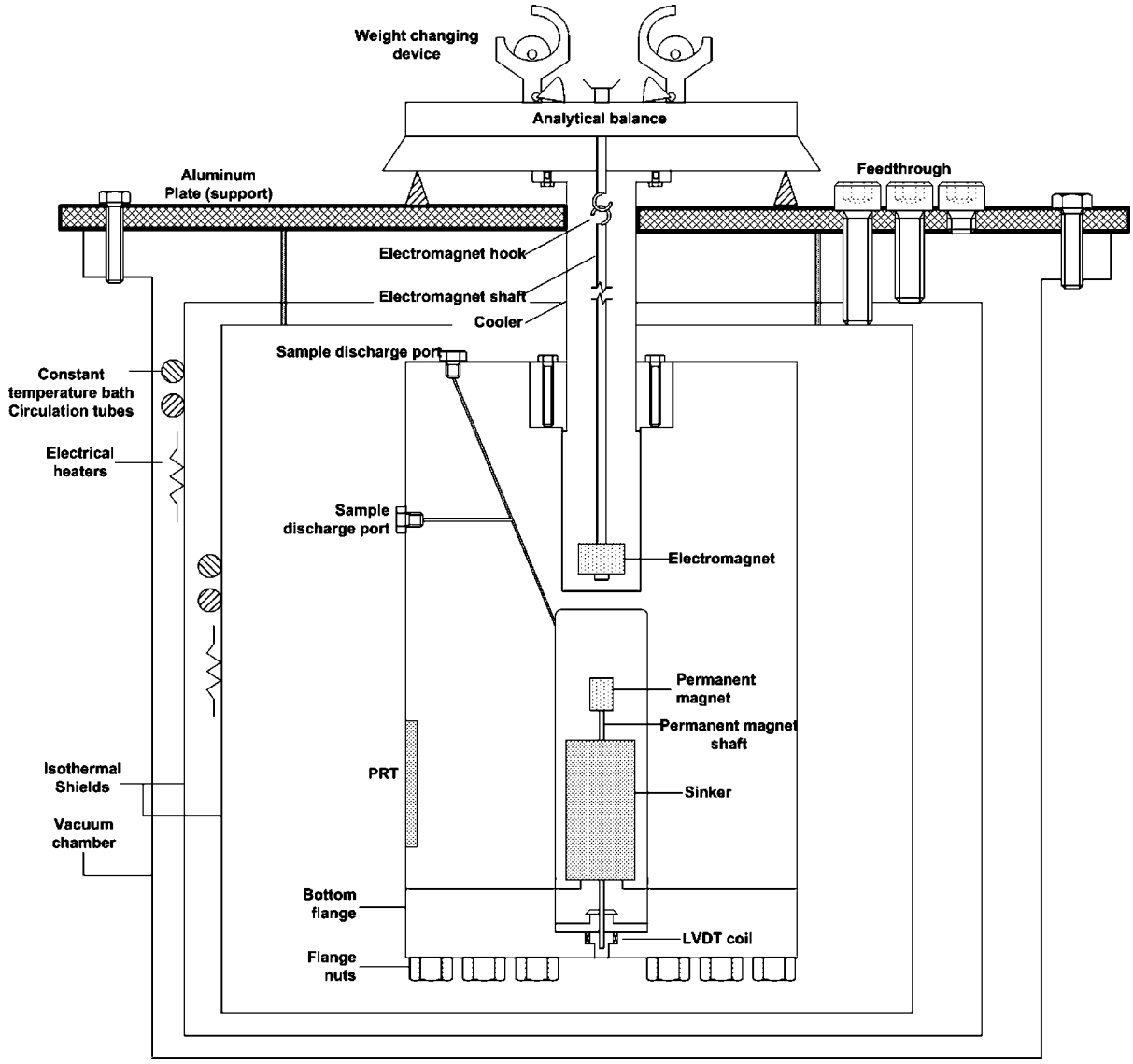

Figure 3. Schematic of high-pressure density cell.

suspension coupling was that it used nonphysical-contact force transmission between the sinker in the pressurized cell and the weighing balance in the atmosphere. This arrangement allowed a cell design that covered a very wide temperature and pressure range.[43]

In a single-sinker MSD, the apparent mass of the sinker is measured while being levitated via a suspension coupling in the pressure vessel at a fixed temperature and pressure. Rubotherm Präzisionsmesstechnik manufactured the compact, single-sinker densimeter used in this work. The apparatus has an uncertainty specification from the manufacturer of 0.005 $kg \cdot m^{-3}$ for densities in the range (0 to 2000) $kg \cdot m^{-3}$ over a temperature range of (193.15 to 523.15) K and a pressure range (up to 200) MPa with a maximum pressure of 130 MPa at 523.15 K. The sinker used for measurements in this work is a titanium cylinder having a volume of 6.74083 ± 0.0034 cm^3 with a 1σ uncertainty of ± 0.05 % in volume and a mass of 30.39157 g, both measured at 293.15 K and 1 bar by the manufacturer. Temperature control utilized a proportional−integral−derivative (PID) mechanism remotely controlled by LabVIEW8.0, and temperature measurements have an uncertainty of 5.7 mK. A coupling and decoupling device couples the sinker magnetically to a commercial analytical balance (Mettler AT 261) with a measuring range of (0 to 62) g with an uncertainty of 0.03 mg.

Since the weighing balance deviates slightly from its ideal operation curve, one must compensate for the nonlinearity of the weighing balance by introducing an external weight compensation system. The balance operates near its zero point to improve the accuracy of the measurement by using two external compensation weights made from titanium and tantalum.[44] Based upon the measurement using the two external weights, eq 2 becomes:

$$\rho = \frac{(m_v + m_{Ti} - m_{Ta}) - (m_a + m_{Ti} - m_{Ta})}{V_s(T,P)} \quad (3)$$

where Ta and Ti are the external Tantalum and Titanium weights. Ta and Ti weights are used to reduce the errors of the balance caused by changes in the characteristic line of the digital balance.[45] Moreover, these Ta and Ti external weights are also used to correct for the effects of air buoyancy on the digital balance.

Table 2. Experimental Pressure and Temperature Points Collected along Isochores

Isochore 1				Isochore 2				Isochore 3			
		ρ	ρ			ρ	ρ			ρ	ρ
T	P	AGA8	GERG	T	P	AGA8	GERG	T	P	AGA8	GERG
K	MPa	kg·m^{-3}	kg·m^{-3}	K	MPa	kg·m^{-3}	kg·m^{-3}	K	MPa	kg·m^{-3}	kg·m^{-3}
343.15	21.053	155.22	155.06	343.15	17.504	130.46	130.34	343.15	15.166	112.95	112.85
333.15	19.911	155.39	155.2	333.15	16.61	130.55	130.41	333.15	14.438	113.07	112.96
323.15	18.768	155.6	155.38	323.15	15.715	130.68	130.51	323.15	13.705	113.19	113.07
313.15	17.62	155.84	155.57	313.15	14.82	130.85	130.65	313.15	12.969	113.33	113.18
303.15	16.463	156.07	155.74	303.15	13.925	131.09	130.85	303.15	12.229	113.48	113.29
293.15	15.299	156.32	155.9	293.15	13.021	131.32	131.01	293.15	11.488	113.69	113.45
283.15	14.145	156.78	156.25	283.15	12.115	131.63	131.23	283.15	10.749	114.02	113.71
278.15	13.562	157	156.4	278.15	11.665	131.88	131.42	278.15	10.375	114.18	113.82
273.15	12.984	157.32	156.65	273.15	11.215	132.18	131.65	273.15	10.007	114.46	114.05
271.15	12.754	157.49	156.78	271.15	11.034	132.3	131.74	271.15	9.861	114.6	114.17
269.15	12.523	157.65	156.9	269.15	10.854	132.44	131.85	269.15	9.711	114.69	114.23
267.15	12.294	157.85	157.06	267.15	10.677	132.64	132.02	267.15	9.563	114.83	114.34
265.15	12.066	158.08	157.25	265.15	10.498	132.83	132.17	265.15	9.418	115.02	114.5
263.15	11.842	158.39	157.52	263.15	10.32	133.05	132.34	263.15	9.272	115.21	114.66
261.15	11.605	158.51	157.59	262.15	10.233	133.2	132.47	261.15	9.125	115.4	114.82
259.15	11.374	158.74	157.78	261.15	10.147	133.37	132.62	259.15	8.976	115.57	114.95
257.15	11.143	158.99	157.98	259.15	9.958	133.43	132.64	257.15	8.829	115.8	115.13
255.15	10.912	159.26	158.19	257.15	9.779	133.68	132.84	256.15	8.757	115.94	115.26
253.15	10.681	159.55	158.43	253.15	9.419	134.21	133.27	254.15	8.617	116.33	115.6
251.15	10.451	159.89	158.71	251.15	9.239	134.52	133.52	253.15	8.551	116.62	115.86
Isochore 4				Isochore 5				Isochore 6			
343.15	12.227	90.119	90.053	343.15	10.008	72.699	72.654	343.15	7.735	55.076	55.048
333.15	11.678	90.147	90.073	333.15	9.592	72.748	72.697	333.15	7.433	55.075	55.044
323.15	11.128	90.188	90.102	323.15	9.177	72.825	72.766	323.15	7.131	55.083	55.046
313.15	10.583	90.304	90.202	313.15	8.76	72.909	72.839	313.15	6.831	55.119	55.076
303.15	10.033	90.412	90.288	303.15	8.338	72.974	72.889	303.15	6.53	55.161	55.11
293.15	9.481	90.548	90.393	293.15	7.917	73.082	72.977	293.15	6.229	55.223	55.16
283.15	8.932	90.788	90.589	283.15	7.497	73.248	73.117	283.15	5.929	55.321	55.244
278.15	8.656	90.924	90.697	278.15	7.285	73.33	73.182	278.15	5.776	55.349	55.263
273.15	8.381	91.102	90.843	273.15	7.075	73.455	73.288	273.15	5.625	55.408	55.313
271.15	8.272	91.198	90.923	271.15	6.991	73.512	73.336	271.15	5.565	55.44	55.34
269.15	8.163	91.3	91.009	269.15	6.909	73.599	73.414	269.15	5.505	55.473	55.369
267.15	8.055	91.425	91.117	267.15	6.825	73.665	73.469	267.15	5.445	55.509	55.4
265.15	7.947	91.559	91.232	265.15	6.742	73.749	73.543	265.15	5.385	55.546	55.433
264.15	7.89	91.582	91.247	264.15	6.7	73.786	73.575	264.15	5.356	55.579	55.463
263.15	7.835	91.639	91.294	263.15	6.659	73.838	73.622	263.15	5.326	55.6	55.481
262.15	7.781	91.714	91.358	262.15	6.62	73.922	73.699	262.15	5.297	55.634	55.513
261.15	7.726	91.775	91.409	261.15	6.58	73.993	73.765	261.15	5.267	55.656	55.532
260.15	7.677	91.937	91.559	260.15	6.541	74.082	73.847	260.15	5.239	55.705	55.579
259.15	7.629	92.122	91.731								
258.15	7.581	92.312	91.909								
Isochore 7				Isochore 8							
343.15	5.582	38.854	38.839	343.15	3.329	22.564	22.559				
333.15	5.38	38.851	38.834	333.15	3.217	22.553	22.547				
323.15	5.177	38.844	38.824	323.15	3.105	22.542	22.535				
313.15	4.973	38.833	38.81	313.15	2.992	22.524	22.516				
303.15	4.771	38.844	38.817	303.15	2.881	22.523	22.514				
293.15	4.571	38.882	38.85	293.15	2.769	22.516	22.505				
283.15	4.368	38.904	38.864	283.15	2.658	22.52	22.506				
278.15	4.266	38.914	38.87	278.15	2.601	22.509	22.494				
273.15	4.164	38.927	38.879	273.15	2.546	22.518	22.501				
271.15	4.123	38.931	38.881	271.15	2.522	22.502	22.485				
269.15	4.083	38.947	38.895	269.15	2.5	22.506	22.488				
267.15	4.042	38.952	38.899	267.15	2.477	22.5	22.482				
265.15	4.002	38.97	38.914	265.15	2.455	22.505	22.486				
264.15	3.982	38.979	38.922	264.15	2.444	22.507	22.488				
263.15	3.961	38.977	38.919	263.15	2.433	22.509	22.489				
262.15	3.939	38.963	38.904	262.15	2.421	22.501	22.481				
261.15	3.918	38.961	38.901	261.15	2.41	22.504	22.483				
260.15	3.896	38.947	38.887	260.15	2.399	22.506	22.485				
				259.15	2.387	22.498	22.477				
				258.15	2.375	22.49	22.469				
				257.15	2.362	22.472	22.45				

Isochoric Apparatus Results

The experimental pressure versus temperature data collected along isochores for the mixture appear in Table 2. The experimental phase envelope data for the mixture studied in this work appears in Table 3 and Figure 4. Below $T/T_{\text{cricondentherm}} = 0.85$, $(\Delta T)/T$ is about constant at 0.1 % or less; however, above 0.85 it grows to about 2 % very near to $T_{\text{cricondentherm}}$ (see Figure 5 in ref 35). $\Delta P/P$ is about 0.025

Table 3. Experimental Phase Envelope Data for the Mixture

T/K	*P*/MPa
230.960	8.718
240.170	9.084
249.100	9.154
255.610	8.715
261.370	7.737
263.730	6.682
264.420	5.363
263.690	3.973
259.890	2.396

% below $P/P_{\text{cricondentherm}} = 0.85$ and grows to about 0.23 % as P approaches $P_{\text{cricondentherm}}$ as shown in Figure 6 of ref 35.

Although the relationship between the compositions of natural gases and their phase envelopes is not well-known, Voulgaris has proposed that higher concentrations of methane, ethane, and CO_2 also increase the solubility of heavy hydrocarbons in the vapor phase.[46] On the contrary, nitrogen decreases the mole fraction of heavy hydrocarbons in the vapor phase. Experimental measurements confirm these general trends and show that the solubility of methane and CO_2 in heavy hydrocarbons is higher (7 and 17 times, respectively) than that for N_2.[47,48] A slight increase of concentration for heavy hydrocarbons moves the dew point curve toward higher values of temperature and pressure.

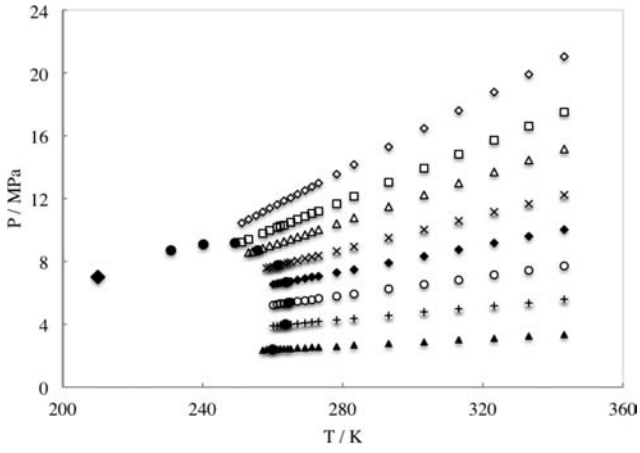

Figure 4. Measured isochores and experimental phase envelope points for the studied sample (●, experimental phase equilibrium point; ◆, estimated critical point for the mixture calculated by PR EOS 208.68 K and 6.46 MPa; ◇, □, △, ×, ◆, ○, +, and ▲ are isochoric experiment points).

Phase envelope calculations performed using various EOS's have significant deviations from the data. EOS calculations for the current mixture appear in Figure 5a−c. Lean mixtures whose structures and properties are apparently simple, such as those reported in this work, can have complex molecular-level effects manifested by the sensitivity of mixture phase envelopes to small variations in concentrations. Cubic EOS fits to the experimental isochoric data use two-parameter versions: Soave−Redlich−Kwong (SRK),[49] Twu−Redlich−Kwong (TRK),[50] Peng−Robinson (PR),[51] and Twu−Peng−Robinson (TPR),[52] as well as three-parameter versions suggested by: Patel−Teja (PT),[53] Patel−Teja−Valderrama (PTV),[54] Schmidt−Wenzel (SW),[55] Guo−Du (GD),[56] and Mohsen-Nia et al. (MMM).[57] Molecular-based EOS's using Wertheim perturbation theory[58] have gained acceptance in academia as the statistical associating fluid theory (SAFT). Since the original SAFT model,[59] several modifications have appeared,[60] one of the most widely accepted being that of Huang and Radosz,[61,62] and one of the most recent being perturbed-chain SAFT (PC-SAFT).[63] Both of these equations have shown promise in industrial applications,[60,63] and this work also uses them for phase envelope predictions. Another molecular-based EOS suggested by Muller et al.[54,58] is the BACKONE EOS. The application of any EOS to multicomponent mixtures requires mixing rules. All extensions of practical EOS to mixtures currently lack exact statistical mechanical guidance.[64] This paper uses the one-fluid mixing rule proposed by van der Waals for cubic EOS and the Berthelot-Lorentz combining rules for a molecular-based EOS in phase envelope calculations.[4,63] Binary interaction parameters required for the calculations come from the literature: Danesh,[4,65] Knapp,[65] or the original EOS references. If none are available, the value is zero.

Magnetic Suspension Densitometer Results

Experimental density results from the single-sinker MSD appear in Table 4. Relative density deviations with respect to AGA8-DC92 EOS and GERG EOS are given in Figures 6 and 7, respectively, in the log−linear scale.[66] Density deviations compared to EOS predictions from AGA8-DC92 indicate that at low temperature and at low pressure the deviations from AGA8-DC92 are greater than those assigned to region 1, which is reported in the original AGA report in 1992 as a lowest uncertainty region. It is clear from these

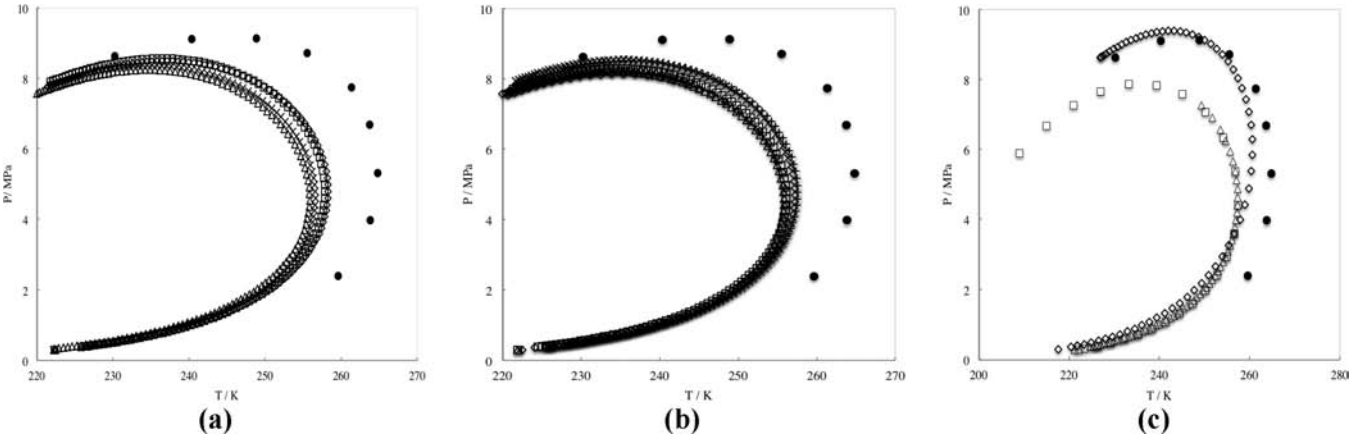

Figure 5. (a) Experimental and predicted phase envelopes of the mixture studied by a biparametric cubic EOS: ●, this work; ◇, SRK; □, TRK; △, PR; ▽, TPR. (b) Experimental and predicted phase envelopes of the mixture studied by a triparametric cubic EOS: ●, this work; ◇, PT; □, PTV; △, SW; ×, GD; +, MMM. (c) Experimental and predicted phase envelopes of the mixture studied by a molecular based EOS: ●, this work; ◇, SAFT; □, PC-SAFT; △, BACKONE.

Table 4. Density Measurements from Single-Sinker Densimeter with a Comparison to the GERG-2004 and AGA8 Models

		density	calculated density					
		exp.	RefProp 8.0[a]	$[(\rho_{exp} - \rho_{theo})/\rho_{theo}]\cdot 100$	GERG04	$[(\rho_{exp} - \rho_{theo})/\rho_{theo}]\cdot 100$	AGA8	$[(\rho_{exp} - \rho_{theo})/\rho_{theo}]\cdot 100$
T/K	P/MPa	kg·m^{-3}	kg·m^{-3}	%	kg·m^{-3}	%	kg·m^{-3}	%
250.076	12.023	190.110	191.030	0.484	190.995	0.465	192.411	1.210
250.019	14.014	219.762	220.304	0.247	220.323	0.255	222.032	1.033
249.999	16.024	242.106	242.203	0.040	242.208	0.042	244.129	0.835
249.968	17.998	259.073	258.813	−0.100	258.775	−0.115	260.859	0.690
249.942	20.033	273.069	272.538	−0.195	272.472	−0.219	274.679	0.590
249.894	21.996	284.284	283.577	−0.248	283.503	−0.274	285.793	0.531
249.978	24.012	293.915	293.063	−0.290	292.991	−0.314	295.327	0.480
250.051	26.003	302.193	301.250	−0.312	301.186	−0.333	303.541	0.446
250.090	27.494	307.793	306.794	−0.324	306.737	−0.343	309.096	0.423
249.986	14.995	231.398	231.827	0.185	231.848	0.195	233.669	0.982
250.033	29.999	316.320	315.337	−0.311	315.294	−0.325	317.641	0.417
250.055	49.993	361.260	360.212	−0.290	360.256	−0.278	362.149	0.246
249.991	68.972	387.532	386.542	−0.255	386.629	−0.233	388.050	0.134
249.997	100.218	417.529	416.623	−0.217	416.737	−0.190	417.550	0.005
249.969	149.856	450.256	449.539	−0.159	449.633	−0.138	449.760	−0.110
349.963	9.975	70.094	70.255	0.229	70.250	0.222	70.290	0.279
349.984	11.967	85.109	85.274	0.193	85.266	0.184	85.322	0.250
350.000	13.958	100.016	100.212	0.196	100.200	0.184	100.275	0.259
349.992	15.985	114.995	115.147	0.133	115.132	0.119	115.226	0.202
350.000	17.955	129.035	129.195	0.124	129.178	0.110	129.291	0.198
350.018	19.959	142.743	142.853	0.077	142.834	0.064	142.965	0.156
349.982	21.940	155.617	155.678	0.039	155.658	0.026	155.807	0.122
349.996	23.914	167.667	167.661	−0.004	167.641	−0.016	167.810	0.085
349.993	25.879	178.859	178.839	−0.011	178.819	−0.023	179.014	0.087
349.996	27.959	189.911	189.857	−0.028	189.836	−0.039	190.067	0.082
349.992	29.877	199.491	199.321	−0.085	199.300	−0.096	199.571	0.040
349.983	9.998	70.244	70.422	0.254	70.418	0.248	70.458	0.304
350.020	29.988	199.950	199.829	−0.060	199.808	−0.071	200.081	0.066
350.030	49.989	269.799	269.336	−0.172	269.323	−0.176	269.968	0.063
349.992	68.941	309.320	308.773	−0.177	308.790	−0.171	309.555	0.076
350.028	99.948	351.590	350.982	−0.173	351.015	−0.163	351.844	0.072
350.012	149.913	395.369	394.763	−0.153	394.732	−0.161	395.641	0.069
450.006	10.054	50.657	50.691	0.068	50.693	0.071	50.711	0.107
450.034	11.969	60.380	60.318	−0.102	60.319	−0.100	60.344	−0.059
450.001	13.976	70.404	70.317	−0.124	70.316	−0.125	70.348	−0.079
450.018	15.961	80.164	80.052	−0.141	80.048	−0.145	80.090	−0.093
450.016	17.971	89.876	89.734	−0.158	89.727	−0.165	89.779	−0.108
449.923	19.975	99.375	99.192	−0.184	99.182	−0.195	99.243	−0.133
449.939	21.977	108.611	108.377	−0.215	108.363	−0.228	108.433	−0.163
449.919	23.985	117.585	117.333	−0.214	117.315	−0.229	117.393	−0.163
449.999	25.976	126.186	125.898	−0.228	125.877	−0.245	125.961	−0.179
449.986	27.979	134.578	134.262	−0.235	134.239	−0.252	134.326	−0.187
449.938	29.978	142.607	142.328	−0.196	142.303	−0.213	142.393	−0.150
449.986	9.994	50.300	50.392	0.182	50.394	0.185	50.412	0.221
450.000	29.976	142.303	142.297	−0.004	142.272	−0.022	142.362	0.042
449.998	49.981	207.882	207.727	−0.075	207.692	−0.092	207.871	−0.005
450.000	68.945	250.899	250.675	−0.089	250.634	−0.105	251.015	0.046
449.989	99.967	299.379	299.074	−0.102	299.025	−0.118	299.581	0.068
450.000	149.899	350.038	349.717	−0.092	349.589	−0.128	350.212	0.050

[a] Calculations made by using neither AGA8 nor GERG-2004 model mixture properties in RefProp 8.0 (options > Preferences>--); user let RefProp 8.0 to calculate the corresponding mixture properties.

results that predictions from AGA8-DC92 and experimental results show deviations at low pressures and low temperatures for the mixture. A closer inspection of samples used for AGA8-DC92 development shows that, except for one mixture, the mole fraction of C_{6+} components does not exceed 0.12 mol %.[67] Among the pure components, AGA8-DC92 development includes mainly methane, ethane, nitrogen, and carbon dioxide. Thus, for any natural gas samples or mixtures with C_{6+} higher than the normal or expanded range, the application of AGA8-DC92 is an extrapolation and the accuracy compared to the normal range is questionable. This work also indicates that AGA8-DC92 fails to predict the density of a simple lean mixture at common operating conditions. It appears that a systematic experimental study is necessary to provide information for developing an EOS for mixtures that include pentanes and C_{6+} fractions.

The total uncertainty of the measurements comes from the uncertainties in pressure and temperature measurements and compositions. The error in density caused by pressure, temperature, and composition is:

$$\Delta\rho = \left\{\left[\left(\frac{\partial\rho}{\partial P}\right)_{T,x}\Delta P\right]^2 + \left[\left(\frac{\partial\rho}{\partial T}\right)_{P,x}\Delta T\right]^2 + \sum_{i=1}^{c}\left[\left(\frac{\partial\rho}{\partial x_i}\right)_{P,T,x_{i\neq j}}\Delta x_i\right]^2\right\}^{1/2} \quad (4)$$

Uncertainties caused by mixture impurities, temperature, and pressure measurements of the measurements are calculated with a 1σ uncertainty of 0.13 %. According to our investiga-

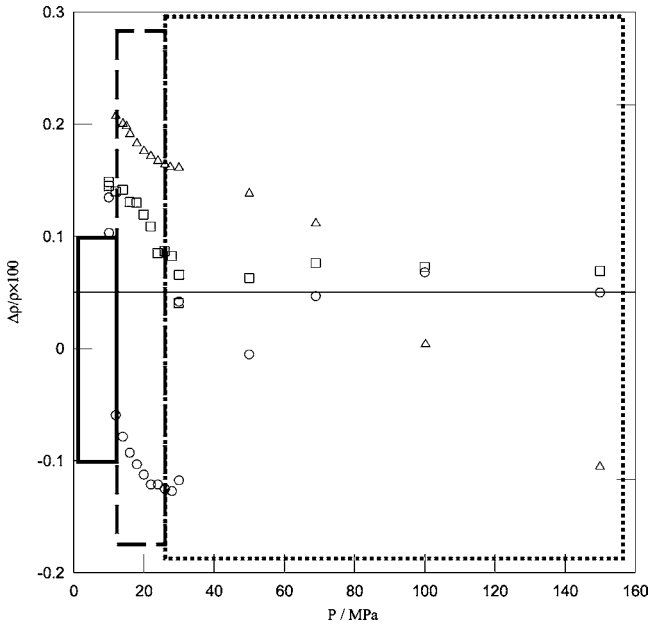

Figure 6. Relative deviations of density data from single-sinker and two-sinker densimeters with respect to the AGA8 equation on a log−linear scale (symbols: △, single-sinker data at 250 K; □, single-sinker data at 350 K; ○, single-sinker data at 450 K; ▲, two-single-sinker data at 250 K; ■, two-single-sinker data at 350 K; ●, two-single-sinker data at 450 K); from left to right: solid line box is AGA uncertainty region 1; long dashed line is AGA uncertainty region 2; fine dashed line is AGA uncertainty region 3.

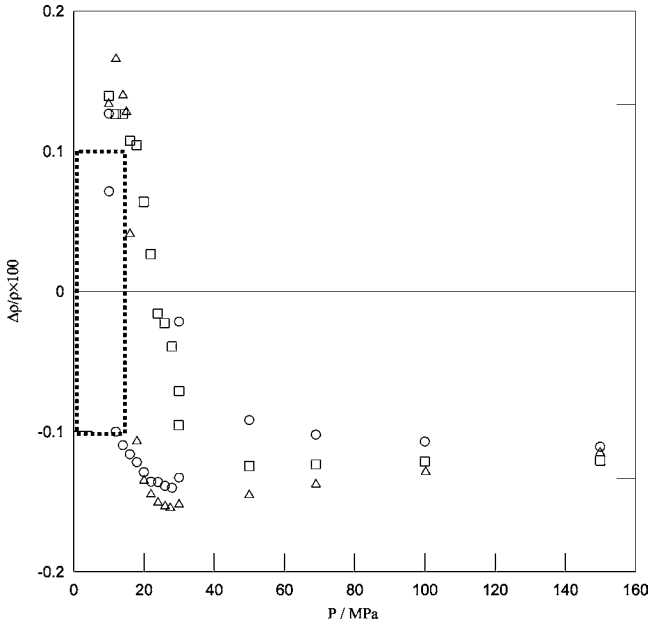

Figure 7. Relative deviations of density data from single-sinker and two-sinker densimeters with respect to the GERG equation in a log−linear scale (symbols: △, single-sinker data at 250 K; □, single-sinker data at 350 K; ○, single-sinker data at 450 K); fine dashed line is the GERG uncertainty region, between (265 to 335) K, and at pressures up to 12 MPa it is ± 0.1 %.

tion, we figured that the effect of temperature, pressure, and the other source of impurities and other uncertainties such as effects of dead volumes near the valves and pressure transducer, buoyancy effect on the external weights in weight changing device, and the volume of the titanium sinker do not dominate the total uncertainty of the measurements. Obviously, the quality of the temperature and pressure sensing equipment used and the frequent calibration of these sensors minimized the total uncertainty effect of both temperature and pressure on density measurements. Moreover, sinker volume calibration has been conducted in NIST, Boulder Laboratories, and we minimized the effect of such uncertainty in our measurements as well. The majority of this uncertainty comes from purity of the pure components that are used during preparing the mixture. We measured the relevant pure components such as nitrogen,[68] carbon dioxide,[69] methane,[70] and ethane[71] prior to mixture measurements, and we performed a measurement performance check with pure components against the well-established related pure component reference EOS. For all of the measured pure components, an experimental uncertainty of $\pm\ 3 \cdot 10^{-4}$ kg·m^{-3} in density is achieved for pressures greater than 7 MPa, and an experimental uncertainty of $\pm\ 5 \cdot 10^{-4}$ kg·m^{-3} in density is achieved for pressures between (5 and 7) MPa.

The MSD yields data with less than 0.03 % relative uncertainty in density over the pressure range of (10 to 200) MPa for nitrogen and carbon dioxide with respect to density measurements and less than 0.05 % relative uncertainty over the same pressure range for methane and ethane with respect to density measurements.

Predictions of pure components via the reference EOS showed better predictive capabilities than reported values in literature as for nitrogen,[72] carbon dioxide,[73] methane,[74] and ethane.[75] The reference EOS for nitrogen[72] has a relative uncertainty with respect to density of 0.02 % over the pressures up to 30 MPa, and at higher pressures the density predictions via a reference EOS agree with the experimental data reported as the 0.05 % deviation band with respect to density. The reference EOS for carbon dioxide[73] has a relative uncertainty of ± (0.03 to 0.05) % with respect to densities below 30 MPa, and at higher pressures, EOS predictions are in agreement with the experimental data with a maximum relative deviation of 0.1 % on density. For methane, reference EOS[74] showed a 0.03 % relative accuracy in density predictions up to 12 MPa and 0.07 % relative accuracy in density predictions up to 50 MPa with respect to experimental data. For ethane, a relative uncertainty of (0.02 to 0.03) % in density up to 30 MPa via a reference EOS[75] was observed.

Conclusions

In this work new and accurate experimental data have been measured for the phase envelopes and the density of a synthetic, light natural gas-like mixture. The effects of mixture composition on phase envelopes reveal that a small fractional increase in the components such as ethane, propane, butane, and pentane produces a remarkable change in the cricondentherm region and near the cricondenbar. N_2 has a smaller effect, but as it increases it moves the cricondentherm toward lower temperatures. Phase envelope predictions by nine cubic and three molecular-based EOS's compared to the data indicate that only SAFT produces reasonable predictions as shown in Figure 6. In particular, SRK, PR, and PT perform poorly for the system studied. Phase envelope predictions from the PR EOS have large deviations with respect to experimental data in both the cricondentherm and the cricondenbar regions. As the long-chain hydrocarbon concentration increases, the PR tends to under-predict the cricondentherm and cricondenbar regions.

The AGA8-DC92 EOS is known to be a very accurate standard for the calculation of the thermodynamic properties of natural gases at typical pipeline conditions, that is, for temperatures of (270 to 330) K at pressures up to 12 MPa. It is believed that the AGA8-DC92 equation shows significant

shortcomings regarding, for example, the range of validity, the uncertainty in the description of natural gases at temperatures below 290 K, and mixtures of unusual composition. In our previous work, we showed the performance of AGA8-DC92 EOS for a mixture that includes unusual compositions such as heavy components of nonane, decane, and some other aromatics.[76] In this work, we compared the density prediction performance of both EOS's for a typical lean natural gas mixture that does not include hexane and heavier components. We have show that GERG EOS shows a little better predicting performance when compared with the AGA8-DC92 EOS within the proposed predicting ranges for both EOS. However, the difference between both EOS's is not dramatic, and for GERG EOS to substitute AGA8-DC92 EOS and become a new industry standard for natural gas density calculations, more experimental work is required, especially at higher pressures and temperatures.

Literature Cited

(1) *International Energy Outlook Report*, DOE/EIA-0484; U.S. Department of Energy: Washington, DC, 2007.

(2) Worldwide Look at Reserves and Production. *Oil Gas J.* **2005**, *103*, 24−25.

(3) Atilhan, M. High Accuracy *P*-ρ-*T* Measurements Up To 200 MPa Between 200 and 500 K Using a Compact Single Sinker Magnetic Suspension Densitometer For Pure And Natural Gas Like Mixtures. Ph.D. Dissertation, Texas A&M University, College Station, TX, 2007.

(4) Danesh, A. *PVT and phase behavior of petroleum reservoir fluids*; Elsevier: Amsterdam, 1998.

(5) Nasrifar, K.; Bolland, O. Predicting Natural Gas Dew Points from 15 Equations of State. *Energy Fuels* **2005**, *19*, 561–572.

(6) Raal, J. D. *Phase Equilibria: Measurement and Computation*; Taylor and Francis: London, 1998.

(7) Moser, B.; Kistenmacher, H. An analysis of the industrial use of a phase equilibria prediction model based on thermodynamic perturbation theory. *Fluid Phase Equilib.* **1987**, *34*, 189–201.

(8) Zhou, J. J.; Patil, P.; Ejaz, S.; Atilhan, M.; Holste, J. C.; Hall, K. R. (*p*, *V*-m, *T*) and phase equilibrium measurements for a natural gas-like mixture using an automated isochoric apparatus. *J. Chem. Thermodyn.* **2006**, *38*, 1489–1494.

(9) Starling, K. E.; Luongo, J. F.; Hubbard, R. A.; Lilly, L. L. Inconsistencies in dew points from different algorithm types possible causes and solutions. *Fluid Phase Equilib.* **2001**, *183*, 209–216.

(10) Avila, S.; Blanco, S. T.; Valeresco, I.; Rauzy, E.; Otn, S. Thermodynamic Properties of Synthetic Natural Gases. 1. Dew-Point Curves of Synthetic Natural Gases and Their Mixtures with Water and Methanol. Measurement and Correlation. *Ind. Eng. Chem. Res.* **2002**, *41*, 3714–3721.

(11) Jarne, C.; Avila, S.; Blanco, S. T.; Rauzy, E.; Otín, S.; Velasco, I. Thermodynamic Properties of Synthetic Natural Gases. 5. Dew Point Curves of Synthetic Natural Gases and Their Mixtures with Water and with Water and Methanol: Measurement and Correlation. *Ind. Eng. Chem. Res.* **2004**, *43*, 209–217.

(12) Fall, J. L.; Luks, K. D. Liquid-liquid-vapor phase equilibria behavior of certain binary carbon dioxide + n-alkylbenzene mixtures. *Fluid Phase Equilib.* **1986**, *28*, 87–96.

(13) Frørup, M. D.; Jepsen, J. r. T.; Fredenslund, A.; Rasmussen, P. High pressure dew and bubble points from microwave measurements. *Fluid Phase Equilib.* **1989**, *52*, 229–235.

(14) Daridon, J. L.; Lagrabette, A.; Lagourette, B. Speed of sound, density, and compressibilities of heavy synthetic cuts from ultrasonic measurements under pressure. *J. Chem. Thermodyn.* **1998**, *30*, 607–623.

(15) May, E. F.; Edwards, J. T.; Mann, G. A.; Miller, C. R. *Development of an automated phase behaviour measurement system for lean hydrocarbon fluid mixtures, using re-entrant rf/microwave resonant cavities*; Elsevier: Amsterdam, Netherlands, 2001; p 406.

(16) May, E. F.; Miller, R. C.; Shan, Z. Densities and Dew Points of Vapor Mixtures of Methane + Propane and Methane + Propane + Hexane Using a Dual-Sinker Densimeter. *J. Chem. Eng. Data* **2001**, *46*, 1160–1166.

(17) Lŏpez, E. R.; Daridon, J. L.; Baylaucq, A.; Ferńandez, J. Thermophysical Properties of Two Poly(alkylene glycol) Derivative Lubricants from High Pressure Acoustic Measurements. *J. Chem. Eng. Data* **2003**, *48*, 1208–1213.

(18) Eubank, P. T.; Kreglewski, A.; Hall, K. R.; Holste, J. C.; Mansoorian, H. Density of an equimolar mixture of ethane and methyl chloride. *AlChE J.* **1985**, *31*, 849–856.

(19) Duerte-Garza, H. A.; Holste, J. C.; Hall, K. R.; Marsh, K. N.; Gammon, B. E. Isochoric *pVT* and Phase Equilibrium Measurements for Carbon Dioxide + Nitrogen. *J. Chem. Eng. Data* **1995**, *40*, 704–711.

(20) Atilhan, M. *A New Cubic Equation of State*; Texas A&M University: College Station, TX, 2004.

(21) Botros, K. K. Performance of five equations of state for the prediction of VLE and densities of natural gas mixtures in the dense phase region. *Chem. Eng. Commun.* **2002**, *189*, 151–172.

(22) Gharbi, R.; Elsharkawy, A. M. Predicting the Bubble-Point Pressure and Formation-Volume-Factor of Worldwide Crude Oil Systems. *Pet. Sci. Technol.* **2003**, *21*, 53–79.

(23) Robinson, R. L.; Jacoby, R. H. Correlation of compressibility factors for gas containing nonhydrocarbons. *Proc., Annu. Conv. Nat. Gas Process. Assoc., Tech. Pap.* **1965**, *44*, 18–22.

(24) Robinson, R. L.; Jacoby, R. H. Better compressibility factors. *Hydrocarbon Process. Pet. Refin.* **1965**, *44*, 141–5.

(25) Yarborough, L.; Hall, K. R. How to solve equation of state for Z-factors. *Oil Gas J.* **1974**, *72*, 86.

(26) Dranchuk, P. M.; Purvis, R. A.; Robinson, D. B. *Computer Calculations of Natural Gas Compressibility Factors Using the Standing and Katz Correlation*; Institute of Petroleum Technical Series No. IP 74-008; Institute of Petroleum: London, 1974.

(27) Dranchuk, P. M.; Abou-Kassem, J. H. Calculation of Z Factors for Natural Gas Using Equations of State. *J. Can. Pet. Technol.* **1975**, *14*, 34.

(28) Valderrama, J. O. The State of the Cubic Equations of State. *Ind. Eng. Chem. Res.* **2003**, *42*, 1603–1618.

(29) Twu, C. H.; Sim, W. D.; Tassone, V. *CEP Mag.* **2002**, 58–65.

(30) Aparicio-Martinez, S.; Hall, K. R. Thermodynamic Properties of Light Synthetic Natural Gas Mixtures Using the RK-PR Cubic Equation of State. *Ind. Eng. Chem. Res.* **2006**, 3684–3692.

(31) Starling, K. E.; Savidge, J. L. *Compressibility Factors of Natural Gas and Other Related Hydrocarbon Gases*; American Gas Association: Arlington, VA, 1992.

(32) Span, R. *Multiparameter Equations of State*; Springer: Berlin, 2000.

(33) Jaeschke, M.; Humphreys, A. E. The GERG Databank of High Accuracy Compressibility Factor Measurements. *Groupe European de Recherches Gazieres Technical Monograph 4 (1990)*, Reprinted from Fortschritt-Berichte VDI, Reihe 6 No. 251; VDI-Verlag: Dusseldorf, 1990.

(34) McLinden, M. O. *P*-ρ-*T* behavior of four synthetic natural gas mixtures from (250 to 450) K with pressures up to 37 MPa, unpublished work; NIST: Boulder, CO, 2010.

(35) Acosta-Perez, P. L.; Cristancho, D. E.; Mantilla, I. D.; Hall, K. R.; Iglesias-Silva, G. A. Method and uncertainties to determine phase boundaries from isochoric data. *Fluid Phase Equilib.* **2009**, *283*, 17–21.

(36) Doiron, T.; Behringer, R. P.; Meyer, H. Equation of state of He^3/He^4 mixture near its liquid-vapor critical point. *J. Low Temp. Phys.* **1976**, *24*, 345–363.

(37) Eubank, P. T.; Barrufet, M. A. General conditions of collonearity at the phase boundaries of fluid mixtures. *AIChE J.* **1987**, *33*, 182–1887.

(38) Eubank, P. T.; Joffrion, L. L.; Patel, M. R.; Warowny, W. Experimental densities and virial coefficients for steam from 348 to 498 K with correction for adsorption effects. *J. Chem. Thermodyn.* **1988**, *20*, 1009–1034.

(39) Stouffer, C. E.; Kellerman, S. J.; Hall, K. R.; Holste, J. C.; Gammon, B. E.; Marsh, K. N. Densities of Carbon Dioxide + Hydrogen Sulfide Mixtures from 220 to 450 K at Pressures up to 25 MPa. *J. Chem. Eng. Data* **2001**, *46*, 1309–1318.

(40) Young, W. C.; Budynas, R. G. *Roark's Formulas for Stress and Strain*, 7th ed.; McGraw-Hill: New York, 2002.

(41) Kleinrahm, R.; Wagner, W. Development and Construction of a Density Measurement Apparatus for Measurement of Boiling and Dew Densities of Pure Fluids over the Complete Phase Boundary Curve. *Prog. Rep. VDI J.* **1984**, *3*, 92.

(42) Beams, J. W.; Clarke, A. M. Magnetic Suspension Balance Method for Determining Densities and Partial Specific Volumes. *Rev. Sci. Instrum.* **1962**, *33*, 750–753.

(43) Lösch, H. W. *Development and Design of New Magnetic Suspension Balances for Non-Contact Measurements of Vertical Forces*; Report 3; VDI Verlag: Dusseldorf, 1987.

(44) Klimeck, J.; Kleinrahm, R.; Wagner, W. An accurate single-sinker densimeter and measurements of the (*p*, ρ, *T*) relation of argon and nitrogen in the temperature range from (235 to 520) K at pressures up to 30 MPa. *J. Chem. Thermodyn.* **1998**, *30*, 1571–1588.

(45) Wagner, W.; Kleinrahm, R. Densimeters for very accurate density measurements of fluids over large ranges of temperature, pressure, and density. *Metrologia* **2004**, *41*, S24–S39.

(46) Voulgaris, M. E. Prediction and verification of hydrocarbon liquid drop out of lean natural gas. Thesis, Delft University of Technology, Delft, Netherlands, 1995.

(47) Ashcroft, S.; Isa, M. B. Effect of Dissolved Gases on the Densities of Hydrocarbons. *J. Chem. Eng. Data* **1997**, 1244–1248.
(48) Schouten, J. A.; Rosmalen, R. J. v.; Michels, J. P. J. Condensation in gas transmission pipelines. *Int. J. Hydrogen Energy* **2005**, *30*, 661–668.
(49) Soave, G. Equilibrium constants from a modified Redlich-Kwong equation of state. *Chem. Eng. Sci.* **1972**, *27*, 1197–1203.
(50) Twu, D. B.; Cunningham, J. R.; Coon, J. E. A Cubic Equation of State with a New Alpha Function and a New Mixing Rule. *Fluid Phase Equilib.* **1991**, *69*, 33–50.
(51) Peng, D. Y.; Robinson, D. B. A New Two-Constant Equation of State. *Ind. Eng. Chem. Fundam.* **1976**, *15*, 59–64.
(52) Twu, C. H.; Coon, J. E.; Cunningham, J. R. A new generalized alpha function for a cubic equation of state. Part 2. Redlich-Kwong equation. *Fluid Phase Equilib.* **1995**, *105*, 61–69.
(53) Patel, N. C.; Teja, A. S. A new cubic equation of state for fluids and fluid mixtures. *Chem. Eng. Sci.* **1982**, *37*, 463–473.
(54) Valderrama, J. O. A Generalized Patel-Teja Equation of State for Polar and Nonpolar Fluids and Their Mixtures. *J. Chem. Eng. Jpn.* **1990**, *1990*, 87–91.
(55) Schmidt, G.; Wenzel, H. A. A modified van der Waals type equation of state. *Chem. Eng. Sci.* **1980**, *35*, 1503–1512.
(56) Guo, T. M.; Du, L. A three-parameter cubic equation of state for reservoir fluids. *Fluid Phase Equilib.* **1989**, *52*, 47–57.
(57) Mohsen-Nia, M.; Modarress, H.; Mansoori, G. A. A cubic hard-core equation of state. *Fluid Phase Equilibr.* **2003**, *206*, 27–39.
(58) Wertheim, M. S. Fluids with highly directional attractive forces. I. Statistical thermodynamics. *J. Stat. Phys.* **1984**, *35*, 19–34.
(59) Chapman, W. G.; Gubbins, K. E.; Jackson, G.; Radosz, M. New reference equation of state for associating liquids. *Ind. Eng. Chem. Res.* **1990**, *29*, 1709–1721.
(60) Muller, E. A.; Gubbins, K. E. Molecular-Based Equations of State for Associating Fluids: A Review of SAFT and Related Approaches. *Ind. Eng. Chem. Res.* **2001**, *40*, 2193–2211.
(61) Huang, S. H.; Radosz, M. Equation of state for small, large, polydisperse, and associating molecules. *Ind. Eng. Chem. Res.* **1990**, *29*, 2284–2294.
(62) Huang, S. H.; Radosz, M. Equation of state for small, large, polydisperse, and associating molecules: extension to fluid mixtures. *Ind. Eng. Chem. Res.* **1991**, *30*, 1994–2005.
(63) Tumakaka, F.; Gross, J.; Sadowski, G. Thermodynamic modeling of complex systems using PC-SAFT. *Fluid Phase Equilib.* **2005**, *228*, 89–98.
(64) Orbey, H.; Sandler, S. L. *Modeling Vapor−Liquid Equilibria*; Cambridge University Press: Cambridge, 1998.
(65) Knapp, H. *Vapor-liquid equilibria for mixtures of low-boiling substances*; Scholium Intl: New York, 1982.
(66) Holste, J. C.; Hall, K. R.; Iglesias-Silva, G. A. Log-linear plots for data representation. *AIChE J.* **1996**, *42*, 296–297.
(67) Savidge, J. L.; Beyerlein, S. W.; Lemmon, E. W. *Technical Reference Document for the 2nd ed. of AGA Report No. 8*, topical report No. GRI-93/0181; Gas Research Institute: Des Plaines, IL, 1995.
(68) Mantilla, I. D.; Cristancho, D. E.; Ejaz, S.; Hall, K. R.; Atilhan, M.; Iglesias-Silva, G. A. New $P\rho T$ Data for Nitrogen at Temperatures from (265 to 400) K at Pressures up to 150 MPa. *J. Chem. Eng. Data* **2010**, *55*, 4227–4230.
(69) Mantilla, I. D.; Cristancho, D. E.; Ejaz, S.; Hall, K. R.; Atilhan, M.; Iglesias-Silva, G. A. P-ρ-T Data for Carbon Dioxide from (310 to 450) K up to 160 MPa. *J. Chem. Eng. Data* **2010**, *55*, 4611–4613.
(70) Cristancho, D. E.; Mantilla, I. D.; Ejaz, S.; Hall, K. R.; Atilhan, M.; Iglesia-Silva, G. A. Accurate $P\rho T$ Data for Methane from (300 to 450) K up to 180 MPa. *J. Chem. Eng. Data* **2009**, *55*, 826–829.
(71) Cristancho, D. E.; Mantilla, I. D.; Ejaz, S.; Hall, K. R.; Atilhan, M.; Iglesias-Silva, G. A. Accurate $P\rho T$ Data for Ethane from (298 to 450) K up to 200 MPa. *J. Chem. Eng. Data* **2010**, *55*, 2746–2749.
(72) Span, R.; Lemmon, E. W.; Jacobsen, R. T.; Wagner, W.; Yokozeki, A. A Reference Equation of State for the Thermodynamic Properties of Nitrogen for Temperatures from 63.151 to 1000 K and Pressures to 2200 MPa. *J. Phys. Chem. Ref. Data* **2000**, *29*, 1361–1433.
(73) Span, R.; Wagner, W. A New Equation of State for Carbon Dioxide Covering the Fluid Region from the Triple-Point Temperature to 1100 K at Pressures up to 800 MPa. *J. Phys. Chem. Ref. Data* **1996**, *25*, 1509–1596.
(74) Setzmann, U.; Wagner, W. A New Equation of State and Tables of Thermodynamic Properties for Methane Covering the Range from the Melting Line to 625 K at Pressures up to 100 MPa. *J. Phys. Chem. Ref. Data* **1991**, *20*, 1061–1151.
(75) Bücker, D.; Wagner, W. A Reference Equation of State for the Thermodynamic Properties of Ethane for Temperatures from the Melting Line to 675 K and Pressures up to 900 MPa. *J. Phys. Chem. Ref. Data* **2006**, *35*, 205–266.
(76) Atilhan, M.; Ejaz, S.; Zhou, J.; Cristancho, D.; Mantilla, I.; Holste, J.; Hall, K. R. Characterization of Deepwater Natural Gas Samples. Part 1: 78% Methane Mixture with Heavy Components. *J. Chem. Eng. Data* **2010**, *55*, 4907–4911.

Received for review June 22, 2010. Accepted December 3, 2010. The Texas Engineering Experiment Station and Texas A&M University have provided financial support for which the authors are grateful. S.A. additionally acknowledges the USA-Spain Fulbright Commission and Ministerio de Educación Ciencia (Spain).

JE100676J